Possible protective role of the *ABCA4* gene c.1268A>G missense variant in Stargardt disease and syndromic retinitis pigmentosa in a Sicilian family: Preliminary data

ROSALIA D'ANGELO[1], LUIGI DONATO[1,2], ISABELLA VENZA[3], CONCETTA SCIMONE[1,2], PASQUALE ARAGONA[1] and ANTONINA SIDOTI[1,2]

[1]Department of Biomedical Sciences, Odontoiatric and Morphofunctional Images, University of Messina, I-98125 Messina; [2]Department of Cutting-Edge Medicine and Therapies, Biomolecular Strategies and Neuroscience, Section of Neuroscience, Applied Molecular Genetics and Predictive Medicine, I.E.ME.S.T., I-90139 Palermo; [3]Department of Clinical and Experimental Medicine, University of Messina, I-98125 Messina, Italy

Received October 13, 2016; Accepted February 7, 2017

DOI: 10.3892/ijmm.2017.2917

Abstract. In the wide horizon of ophthalmologically rare diseases among retinitis pigmentosa forms, Stargardt disease has gradually assumed a significant role due to its heterogeneity. In the present study, we aimed to support one of two opposite hypotheses concerning the causative or protective role of heterozygous c.1268A>G missense variant of the *ABCA4* gene in Stargardt disease and in syndromic retinitis pigmentosa. This study was based on a family consisting of three members: proband, age 54, with high myopia, myopic chorioretinitis and retinal dystrophy; wife, age 65, with mild symptoms; daughter, age 29, asymptomatic. After genetic counseling, *ABCA4* and *RP1* gene analysis was performed. The results highlighted an important genetic picture. The proband was found to carry two variant *RP1* SNPs, rs2293869 (c.2953A>T) and rs61739567 (c.6098G>A), and, a wild-type condition for four *RP1* polymorphisms, rs444772 (c.2623G>A) and three SNPs in the 'hot-spot' region, exon 4. The proband's wife, instead, showed an opposite condition compared to her husband: a homozygous mutated condition for the first four SNPs analyzed, while the last two were wild-type. Regarding the *ABCA4* gene, the proband evidenced a wild-type condition. Furthermore, the wife showed a heterozygous condition of *ABCA4* rs3112831 (c.1268A>G). As expected, the daughter presented heterozygosity for all variants of both genes. In conclusion, even though the c.1268A>G missense variant of the *ABCA4* gene has often been reported as causative of disease, and in other cases protective of disease, in our family case, the variant appears to reduce or delay the risk of onset of Stargardt disease.

Correspondence to: Professor Antonina Sidoti, Department of Biomedical Sciences, Odontoiatric and Morphofunctional Images, University of Messina, via C. Valeria 1, I-98125 Messina, Italy
E-mail: asidoti@unime.it

Key words: Stargardt, retina, *ABCA4*, dystrophy, *RP1*, retinitis pigmentosa

Introduction

In the wide horizon of ophthalmologically rare diseases among retinitis pigmentosa forms, Stargardt disease (OMIM #248200) has gradually assumed an important role due to its heterogeneity. Stargardt disease, known also as fundus flavimaculatus in the late onset form, or heredomacular degeneration, causes progressive bilateral decrease in vision between childhood and teenage years, reaching a plateau phase shortly after rapid reduction in visual acuity by the age of 50. Most patients show a decrease of up to 6/60 or worse, reaching a condition called 'legal blindness'. Stargardt patients develop irregularly shaped yellowish-white flecks or spots in the macula, causing decreased central vision. There is usually no problem regarding peripheral vision, and therefore they rarely have issues with bumping into objects when moving around (due to rod apoptosis). In late stages of the disease, the involvement of cones may also induce impairment of color vision. Other symptoms usually include wavy vision, blind spots, blurriness, and difficulty adapting to dim lighting (1). Gene therapy could be a future solution (2). Stargardt disease is an inherited condition mainly autosomal recessive, and the major causative gene involved is *ABCA4* (3), also known as *ABCR* (4). It is located on the short arm of chromosome 1 (1p22), and encodes for a cytospecific member of the ATP-binding cassette (ABC) transporter superfamily, retina photoreceptor specific. The protein consists of two transmembrane domains (TMDs), also known as membrane-spanning domains (MSDs) or integral membrane (IM) domains. It consists of α-helices, embedded in the membrane bilayer, and is an allosteric protein. The sequence and architecture of TMDs are variable, reflecting the chemical diversity of substrates that can be translocated. The nucleotide binding domain (NBD), on the other hand, is located in the cytoplasm and has a highly conserved sequence, and is the site for ATP binding (4). The structural architecture of ABC transporters consists minimally of two TMDs and two NBDs (5).

The protein plays a fundamental role in the visual cycle. To be precise, it is an inward-directed retinoid flipase, which imports substrates from the lumen to the cytoplasmic side of retinal disc membranes. The substrates are all-*trans*-retinaldehyde (ATR) and *N*-retinyl-phosphatidyl-ethanolamine (NR-PE), an intermediate derived from the reaction of ATR with phosphatidyl-ethanolamine (PE) located in disc membranes. ATR, once transported to the cytoplasmic side, is reduced to vitamin A by *trans*-retinol dehydrogenase (tRDH). Then, transferred to the retinal pigment epithelium (RPE), it is converted to 11-*cis*-retinal. Abca4 protein is involved in photoresponse, removing ATR/NR-PE from the extracellular photoreceptor surfaces during bleach recovery. More than 700 mutations in the *ABCA4* gene (OMIM #601691) have been found to cause Stargardt macular degeneration, most of which consist of single nucleotide variants (SNVs). An altered Abca4 protein cannot remove NR-PE from photoreceptor cells, thus it combines with other ATR molecules. This, in turn, leads to condensation, oxidation, hydrolysis and rearrangements. All of these reactions produce the bis-retinoid Di-retinoid-pyridinium-ethanolamine (A2E) (6), among which is lipofuscin, one of the constituents of fatty yellow pigments that builds up in retinal cells (7). This is toxic to the retina, leading to photoreceptor apoptosis and Stargardt macular degeneration progressive vision loss in patients. Different phenotypes are associated with variable residual functions of the protein, due to several variants of the *ABCA4* gene. It is therefore fundamental to analyze the gene in the most complete way, in order to develop a correct differential diagnosis for each case of Stargardt disease. This is one of the most difficult challenges due to the very common overlapping symptoms of the pathology, and contrasting data. An example is provided by the variant of our case study, regarded as a non-pathogenic polymorphism (SNP), as a high-penetrance disease-causing variant, or even as a possible protecting factor. Similar to other pathologies, there is not just one gene implicated in etiopathogenesis, and *ABCA4* could play a strong role in the development of retinitis pigmentosa.

In our hypothesis, the indirect effects of a mutated *ABCA4* could influence the activity of *RP1*, one of the most frequent causative genes of syndromic or non-syndromic retinitis pigmentosa (8). Retinitis pigmentosa 1 (OMIM #180100), the most common form, shows high involvement of the *RP1* gene, located on 8q12. It is an autosomal dominant form with relatively late onset of night blindness, usually by the third decade of life, with slow progression. Characteristic clinical findings include diffuse retinal pigmentation, progressive decrease in recordable ERGs, and concentric visual field loss. Funduscopic findings comprise retinal atrophy, bone-spicule-like pigment deposits, and vascular attenuation (9). Rp1 protein is located in the region of the axoneme of rod and cone photo-receptors. The photo-receptor axoneme begins at the basal body in the distal inner segment and passes through the connecting cilium. It is considered the primary pass for continuous polarized transport of proteins and membrane needed in outer segments to substitute older discs with new ones (10,11). The junction between the connecting cilium and the outer segment is also where disc morphogenesis occurs (12,13). It has been pointed out (14) that *RP1* could play a role in controlling the orientation and organization of outer segment discs. It may function as a connection between newly formed discs and the axoneme, and this interaction helps discs form in the correct orientation and stack up into outer segments. Proteins present in the disc rims, such as Abca4, Rom1 and peripherin are potential candidates for such an interaction (14). In this study, we report the genetic condition of a family where each carry several variants on the *ABCA4* gene and *RP1*.

Materials and methods

Clinical data. The target of our study is a Sicilian family with three members. The proband, 54-year-old father, showed a symptomatology common to syndromic retinitis pigmentosa and Stargardt disease: high myopia and myopic chorioretinitis, irregular astigmatism, incipient cataract and retinal dystrophy. All of these disorders have left the patient severely visually impaired, with a useful visual acuity of 1/20 in both eyes and short perceptions of light and colors since pediatric age. Fundus examination showed peripheral degeneration, an area of vitreous traction and macular thickness reduced in the right eye. The left eye showed degenerative myopia. Pattern evoked potential (PEP) and flash evoked potential (FEP) confirmed typical signs of retinitis pigmentosa, as shown in pattern electroretinogram (PERG) and flash electroretinogram (FERG) (Figs. 1-4). The proband's wife, 65 years of age, showed only a slight reduction in sensitivity on left eye peripheral areas. Their 29-year-old daughter, instead, has revealed no ophthalmologic symptoms (Fig. 5).

Following detailed genetic counseling, *ABCA4* and *RP1* gene analysis was requested. The research followed the tenets of the Declaration of Helsinki and informed consent was obtained from the subjects after explanation of the nature and possible consequences of the study.

ABCA4 and RP1 genotyping. Genomic DNA was extracted from heparinized peripheral blood using the salting out method and then stored in TE buffer (l0 mM Tris-HCI, l mM EDTA, pH 8.0) until analysis. Coding exons (50 for *ABCA4* and 4 for *RP1*, respectively), intron-exon boundaries and promoter regions of the 2 genes were screened using primers designed according to the *ABCA4* and *RP1* published nucleotide sequence of GenBank (accession no. NG_009073.1 and NG_009840.1, respectively).

Polymerase chain reaction (PCR). PCR amplifications were carried out in a 50 μl solution containing $MgCl_2$ (2.5 mM), dNTPs (0.2 mM), 0.2 μl of each primer (10 μM), 0.8 μg of genomic DNA and 1 unit of Euro Taq polymerase (EuroClone Spa Life Sciences Division, Milan, Italy). DNA amplification was performed on a thermal cycler Gene Amp PCR System 2700 (PE Applied Biosystems, Foster City, CA, USA) as follows. After an initial denaturation step at 94˚C for 5 min, the samples were subjected to 35 cycles of amplification consisting of 40 sec of denaturation at 95˚C, 35 sec of annealing and 45 sec of extension at 72˚C. The annealing temperature was optimized for each primer set. A final extension at 72˚C was carried out for l0 min. Following PCR, 5 μl of amplified product was examined by electrophoresis on a 2% agarose gel. PCR of *RP1* (4 exons) and *ABCA4* (50 exons)

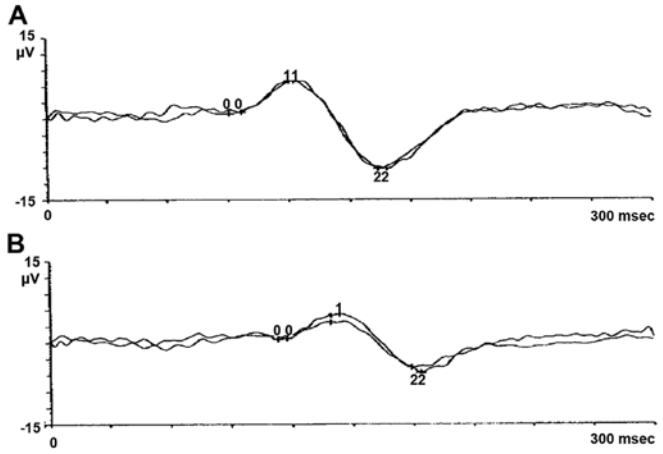

Figure 1. Pattern evoked potential (PEP) for right (A) and left (B) eyes of the proband father. Evoked visual potential morphology was markedly impaired. Component P00 was scarcely detectable. Severe decrease in amplitudes (N75-P100) below normal limits and marked increase in peak times for the P100 component beyond normal limits were noted.

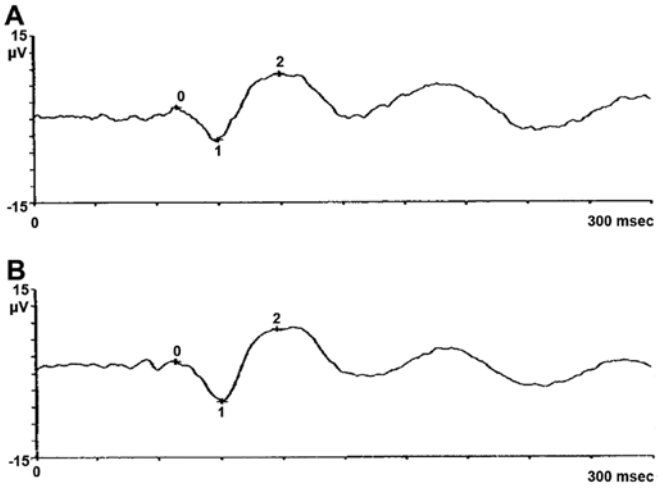

Figure 2. Flash evoked potential (FEP) for right (A) and left (B) eyes of the proband father. Evoked visual potentials of normal morphology, amplitudes (N2-P2) and peak time for the component P2 within the standard limits were noted.

required 12 and 43 primer pairs. See Tables I and II for the sequences of primers.

Sequencing. All PCR products were analyzed also by direct nucleotide sequence analysis by the dideoxynucleotide method with the BigDye Terminator 3.1 Cycle Sequencing kit on the 3500 Genetic Analyzer (Applied Biosystems, Foster City, CA, USA).

Bioinformatic analysis. To clarify the hypothetical effects of the examined variants, a deep bioinformatic analysis with CLC Genomics workbench 8.0.1 (www.clcbio.com) for primary structure details, followed by PSIPRED secondary structure prediction (http://bioinf.cs.ucl.ac.uk/psipred/) was performed. Finally, RaptorX (http://raptorx.uchicago.edu) and Chimera software (http://www.cgl.ucsf.edu/chimera/) were

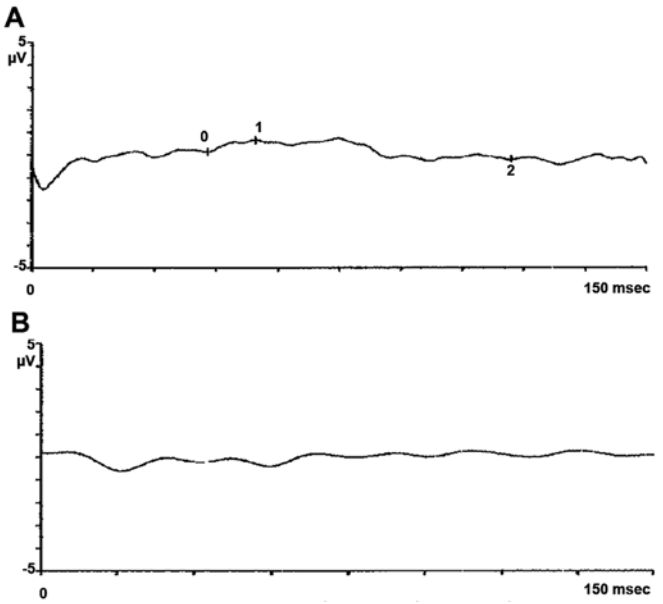

Figure 3. Pattern electroretinogram (PERG) for right (A) and left (B) eyes of the proband father. The first shows severe decrease in amplitude, N35-P50 and P50-N95, lower than normal limits, with an increase in the peak time for the P50 component within normal limits; the second, instead, shows an extinct ERG.

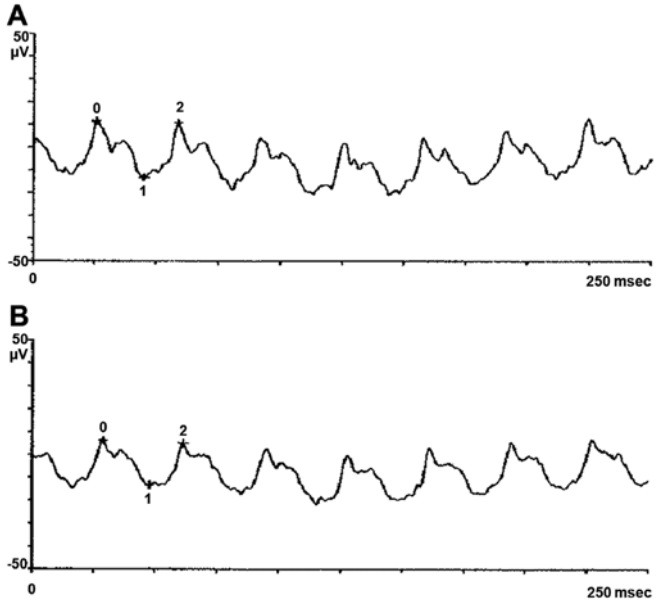

Figure 4. Flash electroretinogram (FERG) for right (A) and left (B) eyes of the proband father. The 30 Hz Flicker response shows a decrease in amplitudes for photopic b-wave below normal limits, while implicit times are standard.

used to highlight third structure aspects of ABCA4-mutated and wild-type predicted proteins.

Results

The entire genotype tree of the family is documented in Fig. 6. Regarding the proband, we report a wild-type condition for rs444772 (c.2623G>A) and for three SNPs of *RP1* 'hot-spot' region in exon 4 (15): rs446227 (c.5008G>A), rs414352 (c.5071T>C) and rs441800 (c.5175A>G). In contrast, we found

Table I. *RP1* primer sequences.

Exon	Forward primer	Reverse primer
1	TGCAGAGCATGCTAGGAACT	TATCAGCATATTGTGAAGGTTG
2	TCTGGATGTCTGCAGCTATAT	AGATGAGATTCCAGTCAGATTCT
3	TGCTCAGTGATGATGTCTTTC	TTTCTGTGGTGGAAGAAACTG
4a	GCTGCCTCTTCCTTTGGATAT	GGCAAACCATTATTATGTGACAT
4b	ATCAAATGGAGGAGTCATCATTA	TCTCAAATACCCAGATGCCACT
4c	CATCCTTGAGCAAAAACCCAA	AGCATCAACTTGACAGAAGCTA
4d	CAAATGCCAGGTTCACTTGCA	TGACATTTTGATGTGACACCAAT
4e	CTTGGATTCAACTGAAGAGTT	AGCCTCTTACTGATTATTTCAT
4f	TTAATACAGTGGTAAATGGA	TGAAATTCCACAGAATTATAA
4g	CATAGGATTTGTTAAAAGGGC	AATAACAGTTAGTATTGGGCAAT
4h	TGTCTCTGATGATGCTATTAAA	TACTGCTTTCAAGATCAGTTAAA
4i	ATCTCAACCAAGTAGTAAGAG	TATATCATCATATAGTCATGCAG

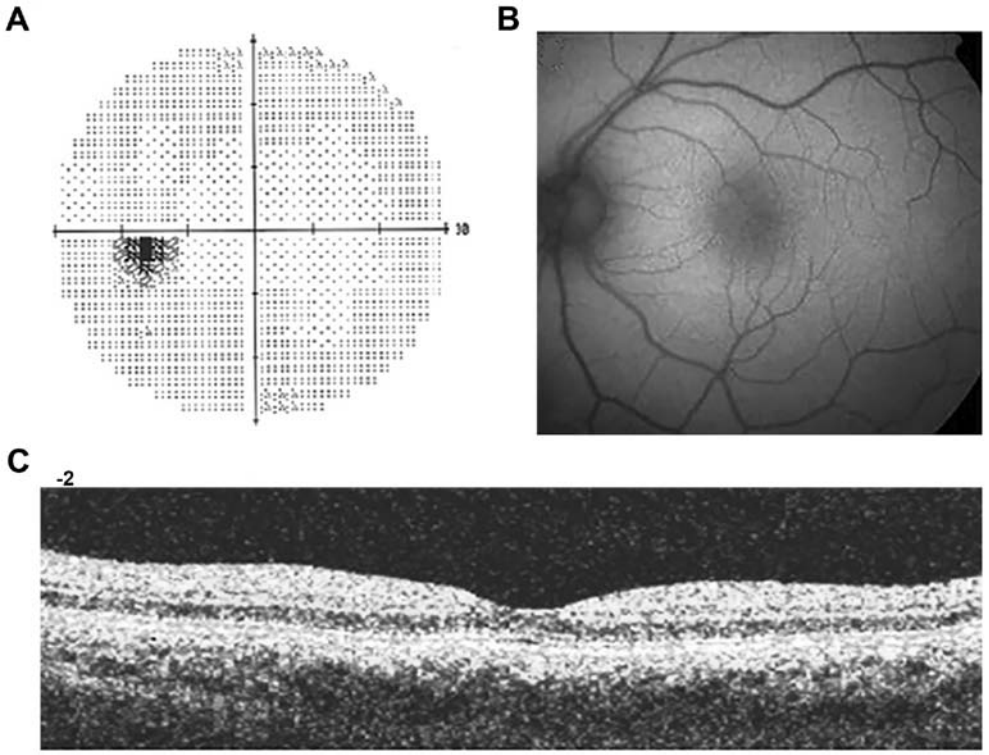

Figure 5. Clinical examination of the proband's daughter: visual field (A), fundus (B) and OCT (C). All of these results highlight a healthy condition.

a homozygous mutated condition regarding the other two *RP1* SNPs, rs2293869 (c.2953A>T) and rs61739567 (c.6098G>A). The proband's wife, instead, showed an opposite situation, a homozygous mutated condition for the first four SNPs analyzed in her husband, while the last two were wild-type. Their daughter, as expected from the parents' genotypes, showed a heterozygous condition for all examined SNPs. Regarding the *ABCA4* gene, the proband showed a wild-type condition for rs3112831 (c.1268A>G), while his wife and daughter were both heterozygous.

We performed a search for Pfam domains on an Abca4-mutated protein sequence, against a wild-type sequence using CLC Genomics Workbench. The Pfam database, a large collection of protein families, each represented by multiple sequence alignments and hidden Markov models (HMMs), delivered the results shown in Table III. The rs3112831 implies that one of two TMD domains starts from aa 515 instead of 513 of the wild-type, altering the recognition site of the protein substrate (ATR or NR-PE).

Examining the micromolecular meanings of these alterations further, a deeper study with many bioinformatic analyses and predictions of primary, secondary and tertiary structures helped us visualize the potentially altered functions of Abca4. Starting from a complete protein report from CLC Genomics

Table II. *ABCA4* primer sequences.

Exon	Forward primer	Reverse primer
1	AACTAAGGGCTTATGTGTAAT	CACTGCTTCAGTGCTAATC
2	TCCTACTGCACACATGGGATC	TTACATGCATCATAGACATGA
3	ACACATGAGATGCTCCTGCT	TCTGCTCCTAAGAGGTTAG
4	TGTAAGGATACTCAATGTAGT	TTCACCAAGGTGATGTTCAA
5	AGTTGAGTTACAAGTGTTTCC	TGAATGTGAACACAAGGAAG
6	GATCTTAATTCCTGTCGCCA	AAGGATTGTCCAGAACACCA
7	AACATATAGGAGATCAGACTG	TTGGGATGTGAACAGGTGCT
8	TAAGGCTCATCCTAGTATTCT	GTTCATGTCCAGAATTGCT
9	TGCTACTAATGATGAGCTTGT	CAGTGATGACTGTGGATGG
10	CCATCCACAGTCATCACTG	TGATCTAACTCCAATAGCG
11	CGCTATTGGAGTTAGATCA	AGACCACTTGACTTGCTAA
12-13	ACCAGACTCTGGAGTTAAGC	CATTAGCGTGTCATGGAGG
14	AGAGTCCTCTGGTGGCTAG	CTGCAGACTTGATGATGTG
15	CACATCATCAAGTCTGCAG	AAGCTAGATGTCACGCTCT
16	ACTTGCAACTCCTCTGAGAG	GCTGTTGCTAGTCAGATGT
17	AGGAACTCAGCACATGGAGT	TGAGGAGTCACTGTTGCAT
18	GCTGACCTTACACTGAGAGA	TCAAGTAGAGCCAGTAGGAT
19	CAAGATTATTGGTCTTGCTGT	ATCAGCCATTCATGATCACA
20	AGATTGTGTGATCAGGCTTG	TTCCACACACATGCAGATG
21	AAGCAGTGCCTGGCATATAG	CTCTCTGAATGAATGTCCAC
22	TGGATGTATACACTGGTGCT	TCTGAGCAGCAGAGGCAGA
23-24	ACAGTGAGCATCTTGATTGC	GTGGTTCCTGTACTCAGCT
25	TACAGTATGTAGGAAGCTATG	CTTCAGAATGTGTTCATCGA
26	CACATAATTGATGACAAGCCA	AGGAATGATGGCTTACTAAG
27-28	GCAGACTTGATGGAGCATCA	CTGGTCTCGAACTCAGGTG
29	GATGATTAAGCTACCAGCCT	ACAGAATGTTCTGGTGGCC
30-31	GGCCACCAGAACATTCTGT	CAACGCCTGCCATCTTGAA
32	CAAGCTAGAGATGGTTATTC	CTACTAGATCAAATAGGAAG
33	TCAACTGTGTCATCTGTATG	GCAGCCAGCTTGAACTATA
34	ATCATTGAAGTGAGAACTAG	CTTCTATGGTCTTCTGATAT
35	CATATGACCTGACAACAGGA	ACTTATGTCCTCCAAGAAGA
36-37-38	AGAGAGCTACTAGTAGGCGT	GAATCCTCTCAGGATGTTCA
39	TAGTGGAGTGACAGCTTCAA	CCTGCGGTGCAGTGATTAT
40	GACTAGTGACAGCTTAACATA	CTGGTTATCAGCTTCAGACC
41	ACAGAGTATATACACAGCTAG	ACAGCTGCTACATGTACGAT
42-43	TACTTCATGACCTCCATTGC	AGTGGATGCTCTTCACATAT
44-45	CAGAAGGAAGCAGAAGCAAG	TCTCATGTGGCTAGTGGAAG
46	CAAGTGCTTAGTAGCCACAT	CAACAGAGGAATCTCTTAAC
47	CATGGAAGAATCTGACAGGA	GAGATGCATCTTCAGGATAA
48	TCATTCTGGAGGCGTGAGAT	GTGGATTAAGGCAATGACAG
49-50	CTGTCATTGCCTTAATCCAC	TCTTATCAGCATGATGGCCT
51	ATTCCTGAGCTCAAGTGATC	AACACACCATAGCATCACAG
52	GTAGGACACAAGCCATACCA	GATGTGATGAGGATGTGGTG
53	ACACATCTCGTATGTGTGTC	AAGACTAGTCCATTCACTTC

Workbench 8.0.1, we noted several important statistical differences which reflect the amino acid change (Table IV).

Furthermore, the substitution of the 423 histidine with a proline brings about important changes in electrical properties and solubility: the conjugate acid (protonated form) of the imidazole side chain in histidine has a pKa of ~6.0; when protonated, the imidazole ring bears two NH bonds and has a positive charge, equally distributed between both nitrogens. The distinctive cyclic structure of the proline side chain, instead, gives proline exceptional conformational rigidity,

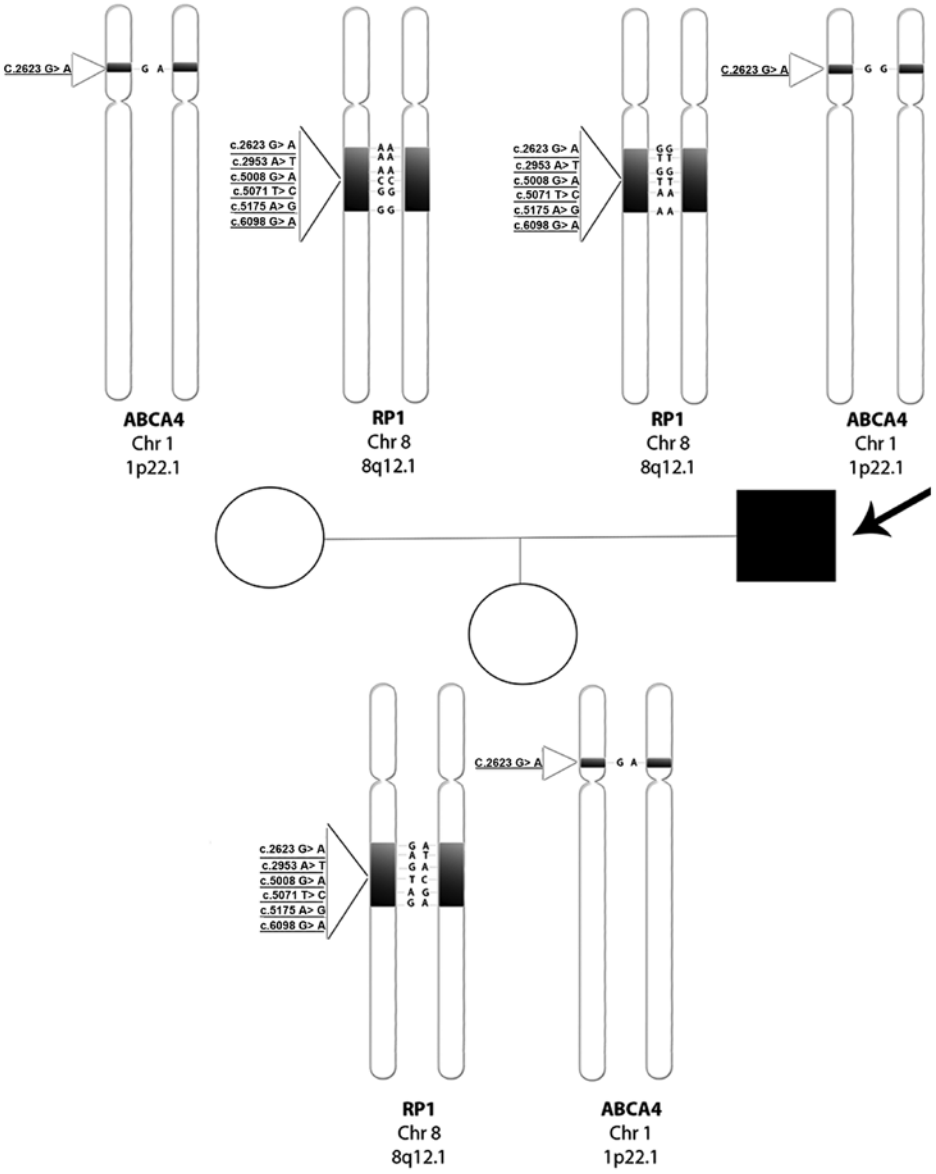

Figure 6. Family tree genotypes for *RP1* and *ABCA4*. Mutated condition, due to present polymorphisms, is underlined. Black arrow indicates the proband.

which affects the rate of peptide bond formation between proline and other amino acids. When proline is bound as an amide in a peptide bond, its nitrogen is not bound to any hydrogen, meaning it cannot act as a hydrogen bond donor, but can be a hydrogen bond acceptor. Figs. 7 and 8 show these differences.

In order to highlight changes in the secondary structure of Abca4, we chose PSIPRED (16), a popular structure prediction method that incorporates two feed-forward neural networks to perform an analysis of results obtained by the PSI-Blast homology search algorithm (17). The resulting scheme (Fig. 9) underlines how the 423H>P causes the substitution of a coil segment between position 504-505 with a helix, probably determining a spatial misfolding which affects the protein function.

Since ATP binding triggers NBD dimerization, the formation of the dimer may represent the 'power stroke'. Rotation and tilting of transmembrane α-helices may both contribute to these conformational changes, so it becomes a crucial forecast whether the examining variant can modify the tertiary structure. RaptorX (18-20) is a protein structure prediction server excelling at predicting 3D structures for protein sequences without close homologs in the Protein Data Bank (PDB). Given an input sequence, RaptorX predicts its secondary and tertiary structures as well as solvent accessibility and disordered regions. We used this web-based application to carry out our aim, and Chimera software (21) to get a detailed 3D picture of the predicted mutated Abca4 from RaptorX pdb exported files (Fig. 10). We hypothesize that the basic N of imidazole side chain acts as a nucleophile towards ATR or NR-PE atoms, constituting a crucial component of the recognition site of Abca4. The substitution of histidine with proline, due to atomic features of the latter, does not permit a correct interaction with ligands: when proline is bound as an amide in a peptide bond, its nitrogen is not bound to any hydrogen, meaning it cannot act

Table III. Pfam protein domain prediction for wild-type and mutated Abca4.

Sequence	Domain	Start	End	Accession	Score	E-value	Description	Predicted by
ABCA4 wild-type	ABC2_membrane_3	1597	1895	PF12698.2	136.4	1.1E-39	ABC-2 family transporter protein	HMMER 3.1b1 (May 2013)
	ABC_tran	946	1090	PF00005.22	105.3	2.9E-30	ABC transporter	HMMER 3.1b1 (May 2013)
	ABC_tran	1955	2099	PF00005.22	74.5	9.1E-21	ABC transporter	HMMER 3.1b1 (May 2013)
	ABC2_membrane_3	**513**	856	PF12698.2	61.1	8.6E-17	ABC-2 family transporter protein	HMMER 3.1b1 (May 2013)
ABCA4 rs3112831 (c.1268A>G)	ABC2_membrane_3	1597	1895	PF12698.2	136.4	1.1E-39	ABC-2 family transporter protein	HMMER 3.1b1 (May 2013)
	ABC_tran	946	1090	PF00005.22	105.3	2.9E-30	ABC transporter	HMMER 3.1b1 (May 2013)
	ABC_tran	1955	2099	PF00005.22	74.5	9.1E-21	ABC transporter	HMMER 3.1b1 (May 2013)
	ABC2_membrane_3	**515**	856	PF12698.2	61.2	8.3E-17	ABC-2 family transporter protein	HMMER 3.1b1 (May 2013)

Main differences between the wild-type and mutated Abca4 domain are shown. Bold font indicates that the ABC2_membrane_3 domain in the mutated protein starts from aa 515 instead of aa 513 in the wild-type protein, due to the rs3112831 polymorphism.

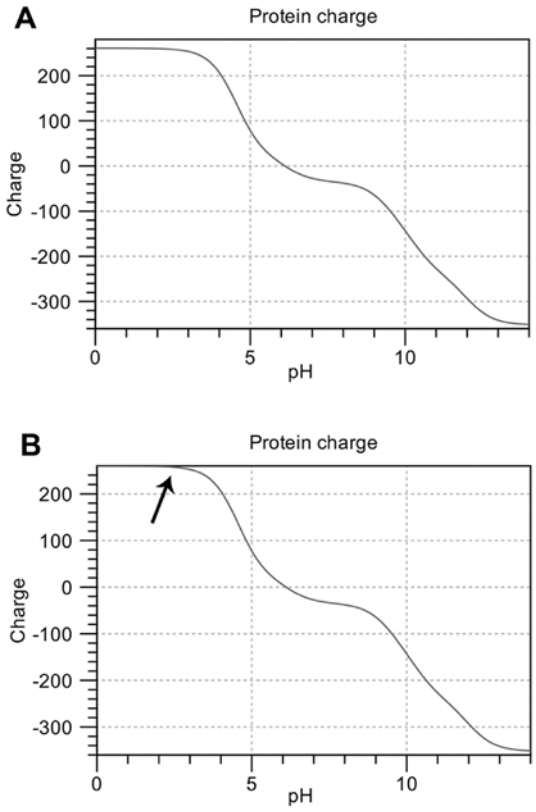

Figure 7. Plot of electrical charge as a function of pH of wild-type (A) and mutated (B) Abca4. Arrows mark the increase in charge at the lowest pH in position 423 for mutated Abca4.

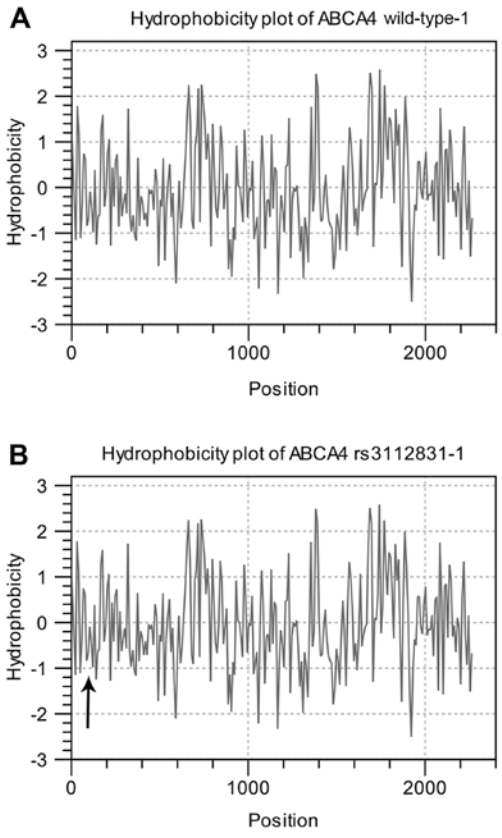

Figure 8. Hydrophobicity plot of wild-type (A) and mutated (B) Abca4. Arrows mark a lower hydrophobicity in position 423 for mutated Abca4.

as a hydrogen bond donor. In Fig. 11, we can see the entire predicted 3D structure of Abca4 before dimerization and all domains, emphasizing the 'transport channel' which involves the 423H>P substitution.

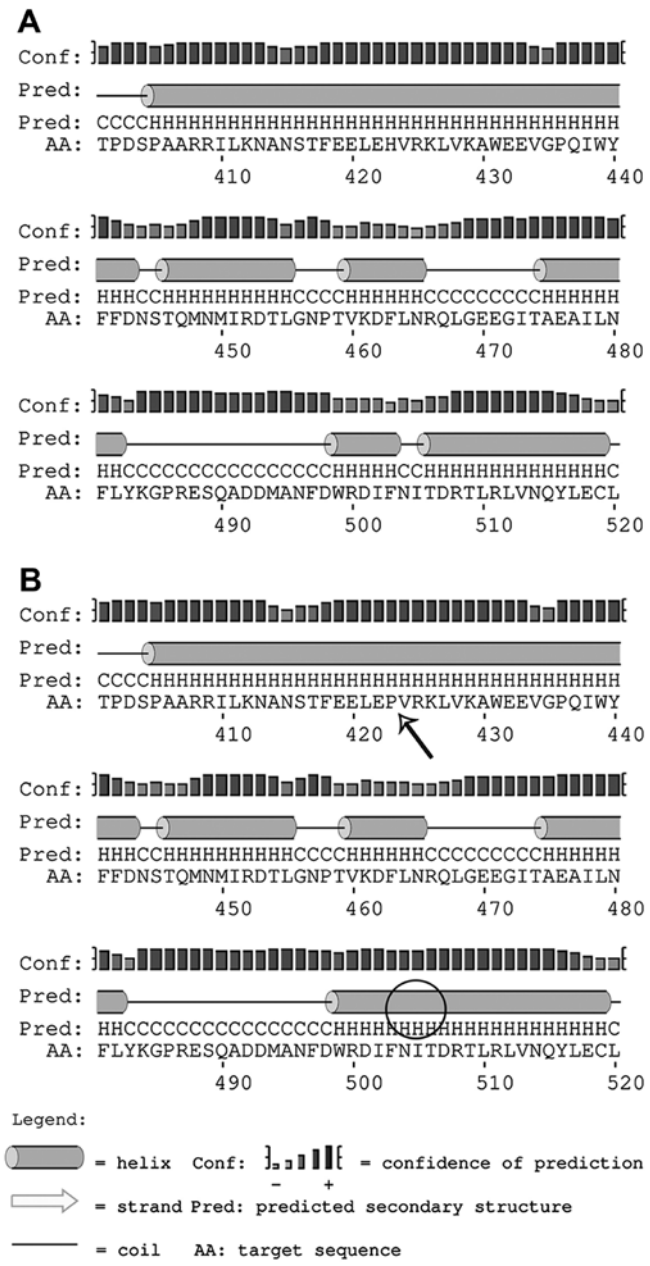

Figure 9. PSIPRED secondary structure of wild-type (A) and mutated (B) Abca4. The 423 H>P substitution induces the insertion of a helix tract for a coiled tract in position 504-505 (evidenced in the circle).

Table IV. CLC Genomics Workbench Abca4 wild-type and mutated Protein Statistic Report.

	Wild-type	rs3112831 (c.1268A>G)
Sequence informations		
Weight (kDa)	255,941	255,901
Isoelectric point	6.12	6.1
Atomic composition		
Carbon (C)	11.588	11.587
Nitrogen (N)	3.039	3.037
Count of hydrophobic and hydrophilic residues		
Hydrophobic (A, F, G, I, L, M, P, V, W)	1.183	1.184
Other	503	502
Amino acid distribution table		
Histidine (H)	52 (0.023)	51 (0.022)
Proline (P)	129 (0.056)	130 (0.057)
Counts of di-peptides		
Glu-His	6 (0.03)	5 (0.02)
Glu-Pro	8 (0.02)	9 (0.03)

Discussion

We believe that *RP1* homozygous variants found in the proband could be responsible for his phenotype. His wife, instead, although carrying a triple homozygous in the 'hot-spot' region of *RP1*, normally associated with retinitis pigmentosa pathology (15), was found to be only mildly affected. Regarding the *ABCA4* gene, she was found to carry the c.1268A>G in heterozygosity. The non-affected daughter inherited a condition of heterozygosity for all analyzed variants of both genes, manifesting no typical symptoms of retinal pathologies upon examination.

Online genetic database (EMBASE, ENSEMBL and PUBMED) reports found variants as polymorphisms. The Human Gene Mutation Database (HGMD) classified two of these (c.5008G>A for *RP1* and c.1268A>G for *ABCA4*) as disease-causing mutations with a question mark (DM?), denoting a probable/possible pathological mutation, reported to be pathogenic in the corresponding report, but where the author has indicated that there may be some degree of uncertainty.

The c.5008G>A, present in the wild-type condition in the proband, implies the change of an alanine in position 1670 with a threonine implemented by this variation and represents a regulatory region modification, due to its location in a promoter flanking region. As with other *RP1* analyzed SNPs, it would appear to be implicated in retinitis pigmentosa phenotype of Chinese (22-25) and Indian (26) populations, as well as indicated as a member of the 'hot-spot' high causative region of *RP1* (27).

The c.1268A>G, also found in the wild-type condition in the proband, represents a missense variation, which changes the histidine in position 423 with a proline, and is located within a regulatory region, showing enhancer features, involving one of TMD. It was regarded as a polymorphism found in heterozygosity in 101/440 controls in a comprehensive survey of sequence variation in the *ABCA4* of a German population (28). The same variant presented as a high-penetrance disease-causing variant in a cohort of patients with Stargardt disease in a study in 2004 (29), and as a reducing risk factor more recently, also in a heterozygous model (30-32). Bioinformatic software predictions (Sift, PolyPhen 2, PROVEAN), analyzing non-synonymous coding SNP effects on protein function, give this variant the status of tolerated or neutral. Furthermore, studies suggest c.1268A>G as associated with late-onset Stargardt disease (33), with macular degeneration (34) and with retinitis pigmentosa (35), depending on the severity of the

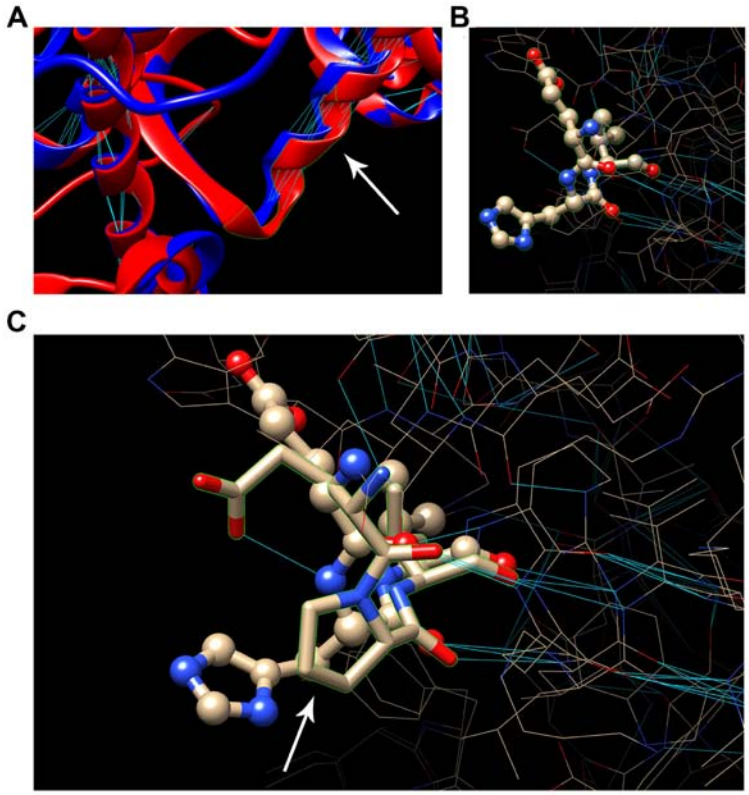

Figure 10. Details of 3D predicted structure of Abca4, using RaptorX web-based application and Chimera software. (A) Arrow indicates the region where 423 amino acid is located; red helix represents wild-type condition, while blue arrow the mutated condition; intramolecular bonds are depicted as colored lines. (B) Ball-and-stick model applied to analyzed the region of Abca4 wild-type predicted structure, with wired version of the surrounding portion represented. (C) Detail of (B), with the addition of the mutated portion of the examined protein region; the arrow focuses attention on proline side chain, as opposed to imidazole side chain of wild-type histidine.

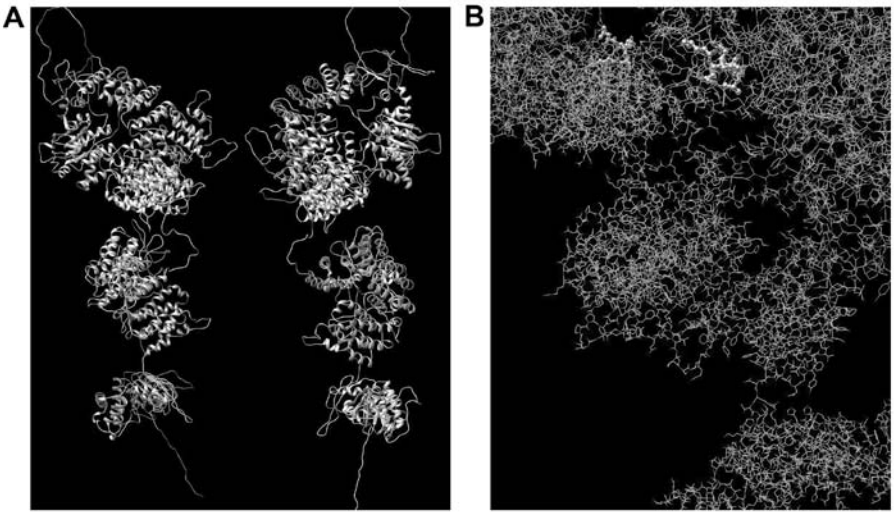

Figure 11. 3D predicted structure of mutated Abca4, using RaptorX web-based application and Chimera software. (A) Predicted structure of the whole Abca4 transporter, before dimerization. Green portions evidence the variant area of each subunit in two transmembrane domains (TMDs). (B) Detail of 'interaction site' which involves the examined mutated region of each subunit and ligands (not shown).

symptoms manifested. Despite all these studies, the phenotype associated with this *ABCA* variant is not clear.

According to our hypotheses, the c.1268A>G missense variant may play a protective role against the damaging *RP1* 'hot-spot' region variants in syndromic retinitis pigmentosa. These findings suggest that, in our family case, the variant examined led to an asymptomatic visual phenotype, without any typical features of Stargardt disease or syndromic retinitis pigmentosa. Our data are corroborated by the genetic (Fig. 6) and phenotypic (only a slight reduction in sensitivity on peripheral areas) condition of the proband's wife and daughter (the latter without any typical or atypical symptomatology), suggesting the likely delaying effect of the analyzed polymorphisms regarding pathology onset. We believe that Rp1 and

Abca4 could interact, directly or indirectly, in order to extend the half-life of photoreceptors. In particular, we speculate that the missense variant 1268A>G of *ABCA4* induces a misfolding into an encoded protein, which decreases the transport of ATR/NR-PE and, consequently, a lower quantity of PE from disc membranes is consumed in spontaneous adduct formation with ATR. This renewed stability of disc membrane lipids could compensate for the lack due to RP1 homozygous variation in the 'hot-spot' region, which results in a misfolded protein unable to guarantee the correct stacking of discs and, above all, proper lipid transport from the inner to the outer segment, in order to build new functional discs.

In conclusion, we analyzed the effects of *ABCA4* rs3112831 in a family with members showing a retinal pathological genotypic condition for ABCA4 and RP1, but without any evidence of phenotypic manifestations. Even thought the c.1268A>G missense variant of the *ABCA4* gene has often been reported as causative of disease, and in other cases protective of disease, in our family case, the variant appears to reduce or delay the risk of onset of Stargardt disease.

References

1. Duno M, Schwartz M, Larsen PL and Rosenberg T: Phenotypic and genetic spectrum of Danish patients with ABCA4-related retinopathy. Ophthalmic Genet 33: 225-231, 2012.
2. Maugeri A, Klevering BJ, Rohrschneider K, Blankenagel A, Brunner HG, Deutman AF, Hoyng CB and Cremers FP: Mutations in the ABCA4 (ABCR) gene are the major cause of autosomal recessive cone-rod dystrophy. Am J Hum Genet 67: 960-966, 2000.
3. Sun H and Nathans J: ABCR: Rod photoreceptor-specific ABC transporter responsible for Stargardt disease. Methods Enzymol 315: 879-897, 2000.
4. Rees DC, Johnson E and Lewinson O: ABC transporters: The power to change. Nat Rev Mol Cell Biol 10: 218-227, 2009.
5. Ambudkar SV, Dey S, Hrycyna CA, Ramachandra M, Pastan I and Gottesman MM: Biochemical, cellular, and pharmacological aspects of the multidrug transporter. Annu Rev Pharmacol Toxicol 39: 361-398, 1999.
6. Jang YP, Matsuda H, Itagaki Y, Nakanishi K and Sparrow JR: Characterization of peroxy-A2E and furan-A2E photooxidation products and detection in human and mouse retinal pigment epithelial cell lipofuscin. J Biol Chem 280: 39732-39739, 2005.
7. Cideciyan AV, Aleman TS, Swider M, Schwartz SB, Steinberg JD, Brucker AJ, Maguire AM, Bennett J, Stone EM and Jacobson SG: Mutations in ABCA4 result in accumulation of lipofuscin before slowing of the retinoid cycle: A reappraisal of the human disease sequence. Hum Mol Genet 13: 525-534, 2004.
8. Pierrottet CO, Zuntini M, Digiuni M, Bazzanella I, Ferri P, Paderni R, Rossetti LM, Cecchin S, Orzalesi N and Bertelli M: Syndromic and non-syndromic forms of retinitis pigmentosa: A comprehensive Italian clinical and molecular study reveals new mutations. Genet Mol Res 13: 8815-8833, 2014.
9. Chang S, Vaccarella L, Olatunji S, Cebulla C and Christoforidis J: Diagnostic challenges in retinitis pigmentosa: Genotypic multiplicity and phenotypic variability. Curr Genomics 12: 267-275, 2011.
10. Young RW: The renewal of photoreceptor cell outer segments. J Cell Biol 33: 61-72, 1967.
11. Anderson DH, Fisher SK and Steinberg RH: Mammalian cones: Disc shedding, phagocytosis, and renewal. Invest Ophthalmol Vis Sci 17: 117-133, 1978.
12. Kinney MS and Fisher SK: The photoreceptors and pigment epithelim of the adult *Xenopus* retina: Morphology and outer segment renewal. Proc R Soc Lond B Biol Sci 201: 131-147, 1978.
13. Steinberg RH, Fisher SK and Anderson DH: Disc morphogenesis in vertebrate photoreceptors. J Comp Neurol 190: 501-508, 1980.
14. Liu Q, Lyubarsky A, Skalet JH, Pugh EN Jr and Pierce EA: RP1 is required for the correct stacking of outer segment discs. Invest Ophthalmol Vis Sci 44: 4171-4183, 2003.
15. El Shamieh S, Boulanger-Scemama E, Lancelot ME, Antonio A, Démontant V, Condroyer C, Letexier M, Saraiva JP, Mohand-Saïd S, Sahel JA, *et al*: Targeted next generation sequencing identifies novel mutations in RP1 as a relatively common cause of autosomal recessive rod-cone dystrophy. Biomed Res Int 2015: 485624, 2015.
16. Buchan DW, Minneci F, Nugent TC, Bryson K and Jones DT: Scalable web services for the PSIPRED Protein Analysis Workbench. Nucleic Acids Res 41: W349-W357, 2013.
17. Altschul SF, Madden TL, Schäffer AA, Zhang J, Zhang Z, Miller W and Lipman DJ: Gapped BLAST and PSI-BLAST: A new generation of protein database search programs. Nucleic Acids Res 25: 3389-3402, 1997.
18. Källberg M, Wang H, Wang S, Peng J, Wang Z, Lu H and Xu J: Template-based protein structure modeling using the RaptorX web server. Nat Protoc 7: 1511-1522, 2012.
19. Ma J, Wang S, Zhao F and Xu J: Protein threading using context-specific alignment potential. Bioinformatics 29: i257-i265, 2013.
20. Peng J, Xu J and Raptor X: RaptorX: Exploiting structure information for protein alignment by statistical inference. Proteins 79 (Suppl 10): 161-171, 2011.
21. Pettersen EF, Goddard TD, Huang CC, Couch GS, Greenblatt DM, Meng EC and Ferrin TE: UCSF Chimera - a visualization system for exploratory research and analysis. J Comput Chem 25: 1605-1612, 2004.
22. Wang DY, Fan BJ, Chan WM, Tam OS, Chiang WY, Lam SC and Pang CP: Digenic association of RHO and RP1 genes with retinitis pigmentosa among Chinese population in Hong Kong. Zhonghua Yi Xue Za Zhi 85: 1613-1617, 2005 (In Chinese).
23. Zhang X, Yeung KY, Pang CP and Fu W: Mutation analysis of retinitis pigmentosa 1 gene in Chinese with retinitis pigmentosa. Zhonghua Yi Xue Yi Chuan Xue Za Zhi 19: 194-197, 2002 (In Chinese).
24. Sheng X, Zhang X, Wu W, Zhuang W, Meng R and Rong W: Variants of RP1 gene in Chinese patients with autosomal dominant retinitis pigmentosa. Can J Ophthalmol 43: 208-212, 2008.
25. Zhang X, Chen LJ, Law JP, Lai TY, Chiang SW, Tam PO, Chu KY, Wang N, Zhang M and Pang CP: Differential pattern of RP1 mutations in retinitis pigmentosa. Mol Vis 16: 1353-1360, 2010.
26. Gandra M, Anandula V, Authiappan V, Sundaramurthy S, Raman R, Bhattacharya S and Govindasamy K: Retinitis pigmentosa: Mutation analysis of RHO, PRPF31, RP1, and IMPDH1 genes in patients from India. Mol Vis 14: 1105-1113, 2008.
27. Schwartz SB, Aleman TS, Cideciyan AV, Swaroop A, Jacobson SG and Stone EM: De novo mutation in the RP1 gene (Arg677ter) associated with retinitis pigmentosa. Invest Ophthalmol Vis Sci 44: 3593-3597, 2003.
28. Rivera A, White K, Stöhr H, Steiner K, Hemmrich N, Grimm T, Jurklies B, Lorenz B, Scholl HP, Apfelstedt-Sylla E, *et al*: A comprehensive survey of sequence variation in the ABCA4 (ABCR) gene in Stargardt disease and age-related macular degeneration. Am J Hum Genet 67: 800-813, 2000.
29. Oh KT, Weleber RG, Stone EM, Oh DM, Rosenow J and Billingslea AM: Electroretinographic findings in patients with Stargardt disease and fundus flavimaculatus. Retina 24: 920-928, 2004.
30. Aguirre-Lamban J, González-Aguilera JJ, Riveiro-Alvarez R, Cantalapiedra D, Avila-Fernandez A, Villaverde-Montero C, Corton M, Blanco-Kelly F, Garcia-Sandoval B and Ayuso C: Further associations between mutations and polymorphisms in the ABCA4 gene: Clinical implication of allelic variants and their role as protector/risk factors. Invest Ophthalmol Vis Sci 52: 6206-6212, 2011.
31. Brión M, Sanchez-Salorio M, Cortón M, de la Fuente M, Pazos B, Othman M, Swaroop A, Abecasis G, Sobrino B and Carracedo A; Spanish multi-centre group of AMD: Genetic association study of age-related macular degeneration in the Spanish population. Acta Ophthalmol 89: e12-e22, 2011.
32. Webster AR, Héon E, Lotery AJ, Vandenburgh K, Casavant TL, Oh KT, Beck G, Fishman GA, Lam BL, Levin A, *et al*: An analysis of allelic variation in the ABCA4 gene. Invest Ophthalmol Vis Sci 42: 1179-1189, 2001.
33. Yatsenko AN, Shroyer NF, Lewis RA and Lupski JR: Late-onset Stargardt disease is associated with missense mutations that map outside known functional regions of ABCR (ABCA4). Hum Genet 108: 346-355, 2001.
34. Baum L, Chan WM, Li WY, Lam DS, Wang PB and Pang CP: ABCA4 sequence variants in Chinese patients with age-related macular degeneration or Stargardt's disease. Ophthalmologica 217: 111-114, 2003.
35. Valverde D, Riveiro-Alvarez R, Aguirre-Lamban J, Baiget M, Carballo M, Antiñolo G, Millán JM, Garcia Sandoval B and Ayuso C: Spectrum of the ABCA4 gene mutations implicated in severe retinopathies in Spanish patients. Invest Ophthalmol Vis Sci 48: 985-990, 2007.